Analysis of compensation principle for wide viewing angle characteristics of an OCB cell by the Poincaré sphere representation

Seong-Ryong Lee*, Tae-Hoon Yoon, and Jae Chang Kim
Department of Electronics Engineering, Pusan National University, Busan, 609-735, Korea
Phone: +82-51-510-1700, E-mail: mengmol@nate.com

Abstract
In this paper, we study how the viewing angle characteristics of a bend cell can be compensated by uniaxial films such as positive a-plate, negative c-plate and circular polarizer. Especially, it is confirmed how the circular polarizer composed of a quarter-wave plate and a linear polarizer enhances the viewing angle characteristics by the Poincaré sphere representation. Also, additional compensation film is designed to improve the viewing angle characteristics of the cell by the Poincaré sphere representation.

1. Introduction
Because of the fast switching time and wide viewing angle properties, the OCB mode is studied as one of the candidates for many display applications such as portable multimedia players and televisions [1-3]. The OCB cells are composed of two polarizers, a bend cell and some retardation films for viewing angle compensation.

Recently, the viewing angle compensation methods of the OCB cells by the circular polarizer have been reported [4-6]. However, only the results of wide viewing angle characteristics were shown without analyzing compensation principle. In this paper we describe how the circular polarizer affects the viewing angle characteristics of the OCB cell by the Poincaré sphere representation (PSR). Also, compensation film is designed to improve the viewing angle characteristics of the OCB cell by PSR.

2. Poincaré sphere representation
The PSR is a powerful tool for analyzing and solving problems involving the propagation of polarized light through birefringent medium [7-9]. Polarization change of a light passing through a birefringent medium can be represented on PS by three steps: 1) calculation and drawing of the PS coordinates, 2) calculation of the rotation axis, and 3) calculation of the rotation angle.

Parameters of each step are obtained by 2X2 extended Jones matrix method as following [8]:

$$\begin{pmatrix} \mathbf{E}_s' \\ \mathbf{E}_p' \end{pmatrix} = \mathbf{T}_o \mathbf{R}(-\psi)\mathbf{P}\mathbf{R}(\psi)\mathbf{T}_i \begin{pmatrix} \mathbf{E}_s \\ \mathbf{E}_p \end{pmatrix} \quad (1)$$

$$\mathbf{P} = \begin{pmatrix} e^{-i\mathbf{k}_{ez}d} & 0 \\ 0 & e^{-i\mathbf{k}_{oz}d} \end{pmatrix} \quad (2)$$

$\mathbf{E}_s$ and $\mathbf{E}_p$ are the amplitudes of the input waves perpendicular and parallel to the plane of incidence, respectively. $\mathbf{E}_s'$ and $\mathbf{E}_p'$ are the amplitudes of the output waves. **s** and **p** indicate unit vectors perpendicular and parallel to the plane of incidence, respectively. The matrix $\mathbf{T}_i$ accounts for the Fresnel refraction of the incident light at the input surface. The rotation matrix $\mathbf{R}(\psi)$ accounts for the transformation that decomposes the light into a linear combination of the normal modes of propagation of the uniaxial medium (i.e. ordinary wave and extraordinary wave). Matrix **P** is the propagation matrix of these normal modes. In the matrix **P**, $\mathbf{k}_{oz}$ and $\mathbf{k}_{ez}$ are the *z*-components of the wave vectors of the ordinary and extraordinary waves inside a uniaxial medium, respectively. The matrix $\mathbf{R}(-\psi)$ transforms the light back into a linear combination of the **s** and **p** waves at the exit of the medium. The matrix $\mathbf{T}_o$ accounts for the Fresnel refraction of the light at the output surface.

The PS coordinates are determined by Stokes parameters, S_1, S_2 and S_3, which depend on the viewing angle. The Stokes parameters are calculated as following [8]:

$$S_1 = E_s^2 - E_p^2 \quad (3)$$

$$S_2 = 2E_s E_p \cos\delta \quad (4)$$

$$S_3 = 2E_s E_p \sin\delta \quad (5)$$

$$S_1^2 + S_2^2 + S_3^2 = 1 \quad (6)$$

where δ means the phase difference between the

electric fileds $\vec{\mathbf{E}}_s$ and $\vec{\mathbf{E}}_p$. The rotation axis and rotation angle are calculated by

$$\psi = -\sin^{-1}\left[\frac{\cos\theta_0 \sin\phi_c \sin\theta_c - \sin\theta_0 \cos\theta_c}{\sqrt{1-\left(\sin\theta_0 \sin\phi_c \sin\theta_c + \cos\theta_0 \cos\theta_c\right)^2}}\right] \quad (7)$$

$$\Gamma_{eff} = \left(k_{ez} - k_{oz}\right)d \quad (8)$$

where θ_c is the angle between the optic axis (OA) and the **z**-axis. ϕ_c is the angle between the projection of the OA on the (**x**, **y**)-plane and the **x**-axis. θ_o is the refraction angle in the uniaxial medium. The wave vector is placed on (y, z)-plane. d is the thickness of the medium. Figure 1 shows PSR drawn by three parameters. The position P and Q represent the polarization state of input and output lights, respectively. The rotation depends on the positive or negative birefringence of the uniaxial medium. If the medium has a positive birefringence, the rotation is clockwise. On the other hand, the rotation is counter-clockwise.

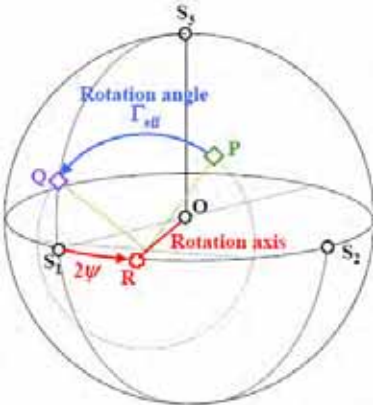

Fig. 1. Parameters of the PSR

3. Structure of the OCB cells

Figure 2 shows the optical configurations of the OCB cells [6]. The LC molecules are aligned at the angle of 0°. The lower circular polarizer consists of a linear polarizer and a QWP whose transmission axis (TA) and OA are oriented at the angles of 45° and 0°, respectively. The OA of positive a-plates and negative c-plates are oriented at the angles of 90° and vertically against the substrate, respectively. The upper circular polarizer consists of a linear polarizer and a QWP whose TA and OA are set to the angles of 135° and 90°, respectively. The positive a-plates are designed to have the same value as that of the bend-cell at the voltage for the dark state and the OA of the positive a-plate is perpendicular to the LC directors. Theoretically, two positive a-plates are used to cancel the retardation value of a bend cell at the normal direction. And two negative c-plates play a role of canceling the effective retardation values of a bend cell and two positive a-plates at the arbitrarily oblique direcitions. In other words, the positive a-plates and negative c-plates are used to make a perfect dark state at the normal and oblique directions, respectively [6]. Δn of the LC is 0.2 and the pretilt angle and the cell gap are 5° and 4.2 um, respectively. The retardation value of a positive a-plate, $R_o=(n_e-n_o)d$, is 38 nm. And that of a negative c-plate [$R_{th}=(n_z-n_o)d$] is 220 nm. The LC director distribution and electro-optical characteristics of the OCB cell are calculated by the commercial software "DIMOS." The voltage of the dark state is fixed at 6 V. Figures 3 (a) and (b) are the iso-contrast ratio lines of the OCB cells without and with QWPs, respectively. Although the effective retardation values of the bend cell are expected to be cancelled by the a- and c-plates at normal and oblique incidence in theory, the viewing angle characteristics are poor without QWPs as shown in Fig 3 (a). However, Fig. 3 (b) shows that the viewing angle characteristics are improved remarkably after the QWPs are inserted between polarizers and negative c-plates, especially at the direction of absorption axes of the crossed polarizers.

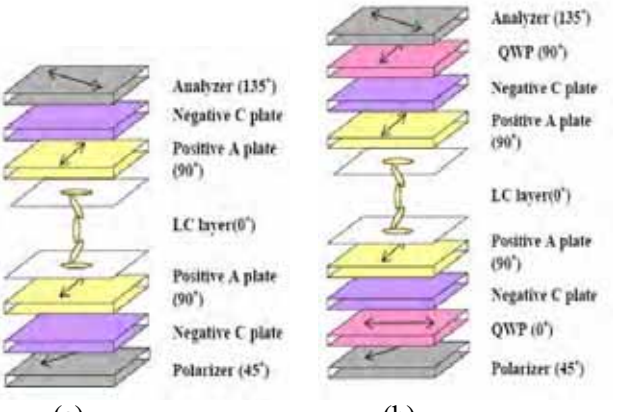

(a) (b)

Fig. 2. Configurations of OCB cell: (a) without, and (b) with QWPs.

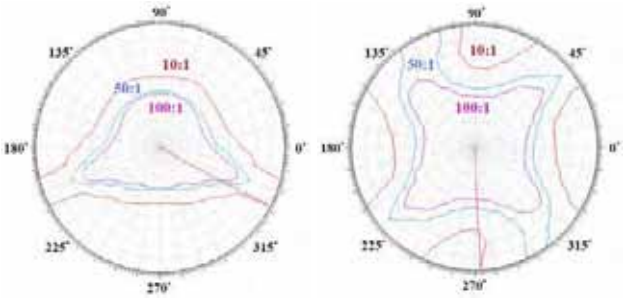

(a) (b)

Fig. 3. Iso-contrast ratio lines: (a) without, and (b) with QWPs.

4. Analysis of viewing angle problems by PSR

The reason for the enhancement can be explained by the PSR. The values of rotation axis and rotation angle are calculated and the traces are drawn on the PS according to each component of the OCB cell in Figs. 4 and 5. LC layer is divided into several slabs and each slab is regarded as uniaxial medium whose optic axis is the direction of LC director. The PSR is performed in two cases of viewing angles whose polar angles are 60° and azimuthal angles are 0° and 45°. In each figure, square box shows the points of analyzer, full dark condition and final polarization state before passing through the analyzer.

Figure 4 shows the PSR at the azimuthal and polar viewing angles of 0° and 60°. In Fig. 4 (a), after the incident light passes through the polarizer, it becomes linealy polarized, and its polarization state is located at point **P**. When such a linearly polarized light passes through the lower negative c-plate, its polarization state is rotated from the point **P** to point $\mathbf{C_1}$ counter-clockwise around the negative $\mathbf{OS_1}$ axis (antipodal axis of the $\mathbf{OS_1}$ axis). When the elliptical polarized light passes through the lower positive a-plate, its polarization state is rotated from point $\mathbf{C_1}$ to point $\mathbf{A_1}$ clockwise around the $\mathbf{OS_1}$ axis. After the light passes through the bend cell, its polarization state is rotated from point $\mathbf{A_1}$ to point **L** counter-clockwise around the $\mathbf{OS_1}$ axis. And after the light passes through the lower positive a-plate and negative c-plate, its polarization state is rotated from point **L** to point $\mathbf{C_2}$ via point $\mathbf{A_2}$ counter-clockwise and clockwise around the negative $\mathbf{OS_1}$ axis and $\mathbf{OS_1}$ axis, respectively. The PSR shows the positive a-plates and negative c-plates are perfectly canceling the effective retardation values of the bend cell as expected. The positive a-plates and negative c-plate are also canceling the effective retardation values of the bend cell after inserting the QWPs as shown in Fig. 4 (b). The points $\mathbf{Q_1}$ and $\mathbf{Q_2}$ indicate the polarization state after passing through the lower and upper QWPs, respectively. The effective retardation values of two QWPs are cancelled each other. However, both of two cases are expected to have the poor dark states because of the light leakages at off-axes of crossed polarizers.

Figure 5 shows the PSR at the azimuthal and polar viewing angles of 60° and 45°. In Fig. 5 (a), after the incident light passes through the polarizer, it becomes linealy polarized, and its polarization state is located at point **P** which corresponds to $\mathbf{S_1}$. When such a linearly polarized light passes through the lower negative c-plate, the polarization state is still located at the same point **P** because the rotation axis is negative $\mathbf{OS_1}$. In other words, lower c-plate does not contribute in canceling the effective retardations of the LC layer and positive a-plates without lower QWP. On the other hand, after QWPs are inserted between linear polarizers and negative c-plates, effective retardation of LC layer is completely eliminated by the positive a-plates and negative c-plates as shown in Fig. 5 (b). It can be said that the QWP plays an important role that other compensation films can perform their parts for enhancing the viewing angle characteristics at this viewing angle.

5. Solution of viewing angle problems by PSR

The viewing angle characteristics are enhanced by the QWPs at the direction of absorption axes of the crossed polarizers. However, the light leaks at the azimuthal and polar viewing angles of 0° and 60°, which correspond to the off-axis of the crossed polarizers. We design a compensation film for diminishing the light leakage. In the PSR, the point of the final polarization state (point **P**) must be moved to near the antipodal point of the output polarizer (point **Q**) by the designed film as shown in Fig. 6 (a). So that, the rotation axis and the rotation angle of the film must be the S_2 axis and 180° in the PSR, respectively. A half-wave biaxial film corresponds to those parameters [10]. The biaxial film is inserted between the upper QWP and analyzer. In Fig. 6 (b), the viewing angle characteristics are enhanced after inserting the film at the off-axis of the crossed polarizer.

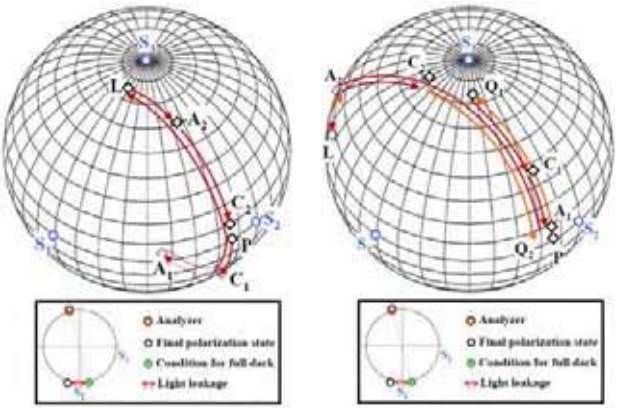

(a) (b)

Fig. 4. PSRs at the azimuthal and polar viewing angles of 0˚ and 60˚: (a) without, and (b) with QWPs.

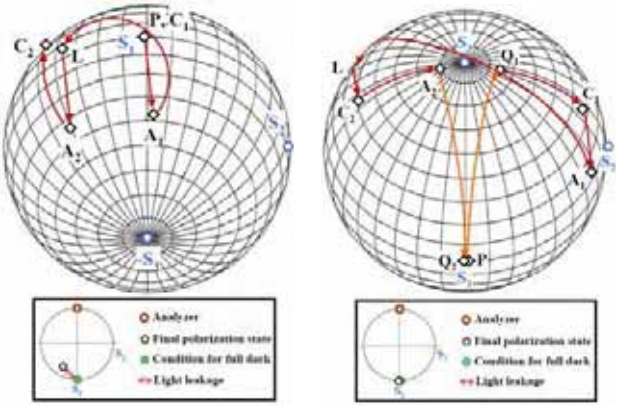

(a) (b)

Fig. 5. PSRs at the azimuthal and polar viewing angles of 45˚ and 60˚: (a) without, and (b) with QWPs.

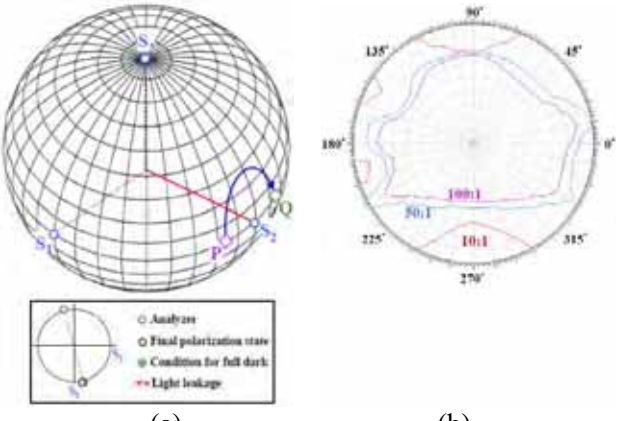

(a) (b)

Fig. 6. Compensation of the light leakage at off-axis direction of the crossed poalrizers: (a) PSR and (b) iso-contrast ratio lines.

6. Summary

The viewing angle characteristics of the OCB cells are analyzed by the PSR. Also, we can design approximately a viewing angle compensation film of the OCB cell by the PSR. As a result of the compensation, the viewing angle characteristics can be enhanced at an arbitrary direction.

7. Acknowledgements

This research was supported by a grant (F0004132) from the Information Display R&D Center, one of the 21st Century Frontier R&D Program funded by the Ministry of Commerce, Industry and Energy of the Korean Government, and by the Second Phase BK21 Program of the Ministry of Education & Human Resources Development, Korea.

8. References

[1] A. Takimoto, K. Nakao and H. Wakemoto, Proc. IDW `04, p. 299, 2004.
[2] Y. Ito, R. Matsubara, H. Mori, and K. Mihayashi, IMID`05 Digest, p. 991, 2005.
[3] N. Koma, T. Miyashita, T. Uchida, and N. Mitani, SID`00 Digest, p. 632, 2000.
[4] T.-J. Chang and P.-L. Chen, Proc. IDW `03, p. 77, 2003.
[5] T. Ishinabe, T. Miysahita, and T.Uchida, SID`04 Digest, p. 641, 2004.
[6] M. J. Jung, C. G. Jhun, J. C. Kim, and T.-H. Yoon, Proc. IDW '04, p. 121, 2004.
[7] J. E. Bigelow and R. A. Kashnow, Appl. Opt. **16**, p.2090, 1977.
[8] K. Vermeirsch, A. D. Meyer, J. Fornier, and H. D. Vleeschouwer, Appl. Opt. **38**, p2775, 1999.
[9] P. Yeh and C. Gu, *Optics of liquid crystal displays* (John Wiley & Sons, Inc., 1999).
[10] J. Chen, K. H. Kim, J. J. Lyu, J. H. Souk, J. R. Kelly, and P. J. Bos, SID`98 Digest, p. 315, 1998.